Last in, first out: the role of cofactor binding the flavodoxin folding.

Bollen, Y.J.M.; Nabuurs, S.M.; Berkel, W.J.H.; van Mierlo, C.P.M.

published in
Journal of Biological Chemistry
2005

DOI (link to publisher)
10.1074/jbc.M412871200

document version
Publisher's PDF, also known as Version of record

THE JOURNAL OF BIOLOGICAL CHEMISTRY
Vol. 280, No. 9, Issue of March 4, pp. 7836–7844, 2005
Printed in U.S.A.

Last In, First Out

THE ROLE OF COFACTOR BINDING IN FLAVODOXIN FOLDING*

Received for publication, November 15, 2004, and in revised form, December 22, 2004
Published, JBC Papers in Press, January 4, 2005, DOI 10.1074/jbc.M412871200

Yves J. M. Bollen‡, Sanne M. Nabuurs, Willem J. H. van Berkel, and Carlo P. M. van Mierlo§

From the Department of Agrotechnology and Food Sciences, Laboratory of Biochemistry, Wageningen University, Dreijenlaan 3, NL-6703 HA Wageningen, The Netherlands

Although many proteins require the binding of a ligand to be functional, the role of ligand binding during folding is scarcely investigated. Here, we have reported the influence of the flavin mononucleotide (FMN) cofactor on the global stability and folding kinetics of *Azotobacter vinelandii* holoflavodoxin. Earlier studies have revealed that *A. vinelandii* apoflavodoxin kinetically folds according to the four-state mechanism: $I_1 \Leftrightarrow$ *unfolded apoflavodoxin* $\Leftrightarrow I_2 \Leftrightarrow$ *native apoflavodoxin*. I_1 is an off-pathway molten globule-like intermediate that populates during denaturant-induced equilibrium unfolding; I_2 is a high energy on-pathway folding intermediate that never populates to a significant extent. Here, we have presented extensive denaturant-induced equilibrium unfolding data of holoflavodoxin, holoflavodoxin with excess FMN, and apoflavodoxin as well as kinetic folding and unfolding data of holoflavodoxin. All folding data are excellently described by a five-state mechanism: I_1 + *FMN* $\Leftrightarrow$ *unfolded apoflavodoxin* + *FMN* $\Leftrightarrow I_2$ + *FMN* $\Leftrightarrow$ *native apoflavodoxin* + *FMN* $\Leftrightarrow$ *holoflavodoxin*. The last step in flavodoxin folding is thus the binding of FMN to native apoflavodoxin. I_1, I_2, and unfolded apoflavodoxin do not interact to a significant extent with FMN. The autonomous formation of native apoflavodoxin is essential during holoflavodoxin folding. Excess FMN does not accelerate holoflavodoxin folding, and FMN does not act as a nucleation site for folding. The stability of holoflavodoxin is so high that even under strongly denaturing conditions FMN needs to be released first before global unfolding of the protein can occur.

Both *in vivo* and *in vitro* the folding of a protein is a complex process. Current knowledge about this process largely stems from *in vitro* studies of small proteins (<20 kDa). The general picture that has emerged is that the topology of the native state is a key factor in determining the rate with which a protein folds (1). In addition, many proteins form one or more metastable intermediates while folding. Some of these intermediates are interpreted to be productive species that accelerate the folding process, whereas others appear to be misfolded conformations (2). The role an intermediate has in kinetic folding also depends to some extent on the experimental conditions used (3).

Many proteins require the binding of a non-covalently bound ligand to be functional. The ligand, or cofactor, can vary from a simple metal ion to a large organic molecule. The influences of cofactor binding on the structure of the protein are manifold. For example, apocytochrome *c* is largely unstructured; it only folds upon incorporation of its heme cofactor (4). In contrast, apoflavodoxin is structurally identical to holoflavodoxin, except for increased dynamics in the region where the flavin cofactor binds (5, 6). The quaternary structure of a protein also can depend on the binding of a cofactor. For example, inactive monomeric apolipoamide dehydrogenase forms active dimers after incorporation of FAD (7).

Although many proteins require the binding of a non-covalently bound ligand to be functional, the role of ligand binding during folding is scarcely investigated. In principle, a ligand could bind to an unfolded protein and reduce the conformational freedom of the polypeptide, thereby reducing the conformational space sampled during protein folding. Such ligands might potentially speed up the folding process by acting as a nucleation site. In some cases, ligands indeed remain bound to the unfolded protein (8, 9). However, in other cases, ligands may not interact with non-native protein states and only become incorporated in the protein during the final stages of protein folding. *In vivo*, chaperones may also play a role in the incorporation of a ligand. As kinetic folding studies of proteins in the presence of their ligands are sparse, the kinetic role of ligand binding during protein folding remains unclear.

Flavoproteins offer a good opportunity to study the role of ligand binding during protein folding. The flavin cofactor is generally non-covalently bound and can be reversibly removed (10). Reconstitution of the holoprotein from its constituents can be studied because of changes in spectroscopic properties that accompany flavin binding.

Here, the influence of the flavin mononucleotide (FMN)[1] cofactor on the folding of the 179-residue *Azotobacter vinelandii* flavodoxin was investigated. Flavodoxins are monomeric proteins (Fig. 1) that function as low potential one-electron carriers in many microorganisms. Both the denaturant-induced equilibrium unfolding and the kinetic folding of *A. vinelandii* apoflavodoxin, *i.e.* flavodoxin in the absence of its cofactor, have recently been studied in great detail (11–14). Apoflavodoxin is structurally identical to holoflavodoxin except for increased dynamics in the flavin binding region (5, 6). Apoflavodoxin kinetic folding can be described by the model shown in Equation 1 (13)

$$I_1 \rightleftarrows U \rightleftarrows I_2 \rightleftarrows N \qquad \text{(Eq. 1)}$$

where U and N are unfolded and native apoflavodoxin, respec-

* The costs of publication of this article were defrayed in part by the payment of page charges. This article must therefore be hereby marked "*advertisement*" in accordance with 18 U.S.C. Section 1734 solely to indicate this fact.

‡ Present address: Dept. of Structural Biology, Faculty of Earth and Life Sciences, Vrije Universiteit, 1081 HV Amsterdam, The Netherlands.

§ To whom correspondence should be addressed. Tel.: 31-317-484621; Fax: 31-317-484801; E-mail: carlo.vanmierlo@wur.nl.

[1] The abbreviations used are: FMN, flavin mononucleotide; GuHCl, guanidinium chloride.

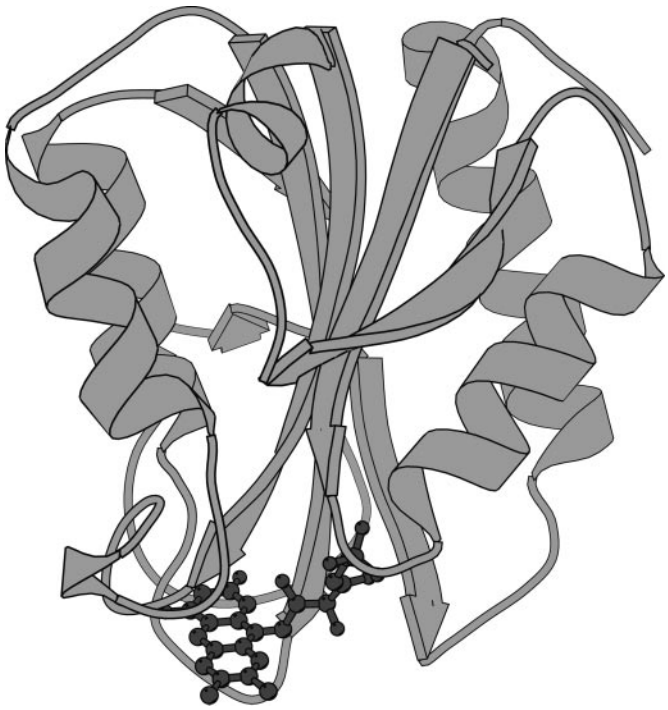

FIG. 1. **Molscript schematic drawing (30) of the x-ray structure of *Azotobacter chroococcum* flavodoxin (31), the sequence of which is 95% identical to *A. vinelandii* flavodoxin.** The secondary structure depicted is based on the NMR spectroscopic data of *A. vinelandii* holoflavodoxin (5). The FMN cofactor is shown in *dark gray* in *ball-and-stick* representation.

tively, and I_1 and I_2 are folding intermediates. During denaturant-induced equilibrium unfolding apoflavodoxin populates the relatively stable folding intermediate I_1, which has molten globule-like characteristics. During kinetic *A. vinelandii* apoflavodoxin folding intermediate I_1 acts as a trap. Intermediate I_1 is off the direct folding route between unfolded and native apoflavodoxin and has to unfold before native apoflavodoxin can be formed. Some folding apoflavodoxin molecules manage to circumvent this trap and fold via a direct and rapid route to the native state, on which the second folding intermediate I_2 is located. This second intermediate is highly unstable and never populates to a significant extent and is thus not observed during denaturant-induced equilibrium unfolding of apoflavodoxin. All folding apoflavodoxin molecules pass through this high energy intermediate before reaching the native state.

In this study we reported on (i) the kinetics of FMN binding to native *A. vinelandii* apoflavodoxin, (ii) the kinetics of FMN binding during *A. vinelandii* holoflavodoxin folding, (iii) the release of FMN during *A. vinelandii* holoflavodoxin unfolding, and (iv) the influence of FMN binding on the global stability of *A. vinelandii* holoflavodoxin. By doing so, the role of FMN during *A. vinelandii* flavodoxin folding was deciphered.

EXPERIMENTAL PROCEDURES

Materials—Guanidinium chloride (GuHCl, ultrapure) and potassium pyrophosphate were from Sigma. In holoflavodoxin equilibrium unfolding experiments, FMN purchased from Sigma was used without further purification. In all other experiments FMN obtained during the preparation of apoflavodoxin (see below) and purified by reverse-phase HPLC was used.

Protein Expression and Purification—Recombinant *A. vinelandii* C69A holoflavodoxin was obtained and purified as described previously (5, 11). The holoflavodoxin concentration was determined spectrophotometrically using an extinction coefficient of 11.3 mM^{-1} cm^{-1} at 452 nm (15). Apoflavodoxin was subsequently prepared by trichloroacetic acid precipitation (11, 16) followed by gel filtration on a Superdex 200 prep grade column (Amersham Biosciences) to remove apoflavodoxin molecules in an oligomeric state (13). The apoflavodoxin concentration was determined spectrophotometrically using an extinction coefficient at 280 nm of 29 mM^{-1} cm^{-1} (17).

Dissociation Constant of the Apoflavodoxin-FMN complex—The dissociation constant of the apoflavodoxin-FMN complex was determined using the quenching of FMN fluorescence upon binding to the apoprotein (18). A solution of 1.5 ml containing 210 nM FMN (based on the extinction coefficient at 445 nm of 12.2 mM^{-1} cm^{-1} (19)) in 100 mM potassium pyrophosphate, pH 6.0, was titrated with aliquots of 4.1 μM apoflavodoxin in the same buffer. After each addition of protein, the system was allowed to equilibrate for 5 min in the dark. Subsequently, the FMN fluorescence intensity was determined using a Cary eclipse fluorimeter equipped with a peltier accessory operating at 25 °C (Varian, Palo Alto, CA). Excitation was at 445 nm with a slit of 5 nm; emission was recorded at 525 nm with a slit of 10 nm. The dissociation constant of the apoflavodoxin-FMN complex was determined by fitting the fluorescence emission to Equation 2, a slightly modified equation compared with the one described in Ref. 19,

$$F = dF_{\text{end}} + F_{\delta}\left(dC_F - \frac{(C_A + K_D + dC_F) - \sqrt{(C_A + K_D + dC_F)^2 - 4C_A dC_F}}{2}\right) \quad \text{(Eq. 2)}$$

where F is the observed fluorescence intensity after each addition, d the dilution factor (initial volume/total volume), F_{end} the remaining fluorescence intensity after the titration (resulting from both fluorescence of holoflavodoxin and traces of flavin impurities that are unable to bind to apoflavodoxin), F_{δ} the difference in molar emission intensity between holoflavodoxin and free FMN, C_F the initial concentration of FMN, C_A the total protein concentration (*i.e.* apo + holo), and K_D the dissociation constant of the apoflavodoxin-FMN complex. The fit resulted in values for C_A that indicate an apoflavodoxin stock solution of 4.4 μM instead of 4.1 μM. As a consequence, an extinction coefficient for *A. vinelandii* apoflavodoxin at 280 nm of 27 mM^{-1} cm^{-1} was used in the rest of this study instead of the value of 29 mM^{-1} cm^{-1} reported elsewhere (17).

FMN Binding Kinetics—Kinetic FMN binding experiments were performed on a BioLogic (Claix, France) SFM-4 stopped-flow apparatus. Solutions were thermostated at 25 °C using a circulating water bath. FMN and apoflavodoxin, both in 100 mM potassium pyrophosphate, pH 6.0, were mixed in different ratios. Pseudo-first-order kinetics were obtained by assuring at least a 10-fold excess of apoflavodoxin relative to FMN. The final FMN concentration was 0.10 μM in all cases, except for the two highest protein concentrations (*i.e.* 10 and 12.5 μM apoflavodoxin) where an FMN concentration of 1.0 μM was used. Binding of FMN to apoflavodoxin was monitored via the accompanying quenching of the FMN fluorescence. The excitation wavelength was 446 nm using an 8-nm slit, and emission was recorded above 475 nm using a cutoff filter. Exponential equations were fitted to the kinetic traces using ProFit (Quantumsoft, Zürich, Switzerland).

Denaturant-induced Equilibrium Unfolding of Holoflavodoxin—Three GuHCl-induced equilibrium unfolding experiments were done: one with apoflavodoxin, one with holoflavodoxin, and one with holoflavodoxin in the presence of 100 μM excess FMN. Unfolding was monitored by circular dichroism (CD) and fluorescence spectroscopy. Before measurements, all samples were equilibrated for at least 12 h at 25 °C in the dark. The protein concentration was 4.0 μM in all cases.

Steady-state far-UV CD measurements were performed on a Jasco J715 spectropolarimeter (Tokyo, Japan) equipped with a PTC-348WI peltier temperature control system. The cell chamber was purged with dry nitrogen gas at a flow rate of 5 liters/min. Calibration was performed with a solution of ammonium d10-camphorsulfonate in nanopure water, the concentration (0.06% w/v) of which was checked spectrophotometrically. GuHCl unfolding samples were measured in a 1-mm quartz cuvette (Starna, Hainault, England) at 222 and 255 nm, and the corresponding signal was averaged over 3 min/wavelength at a temperature of 25 °C. The ellipticity at 255 nm was subtracted from the 222 nm ellipticity as a baseline value. Before and after each measurement series, 222 and 255 nm ellipticity values (θ) of a buffer solution (*i.e.* 100 mM potassium pyrophosphate, pH 6.0) were recorded. The average net buffer ellipticity (*i.e.* $<\theta 222\text{-}\theta 255>$) was subtracted from all sample ellipticities to allow quantitative comparison of ellipticity values that result from different experiments.

Tryptophan fluorescence intensity was determined in a 1-ml quartz cuvette (excitation path length 1 cm) using a Cary eclipse fluorimeter equipped with a peltier accessory operating at 25 °C (Varian). Excita-

tion was at 280 nm with a slit of 5 nm; emission was measured for 5 s at 350 nm with a slit of 2.5 nm. In the presence of 100 μM excess FMN, fluorescence emission was recorded using a 0.5-ml quartz cuvette that was positioned with its long side (1-cm length) perpendicular to the excitation beam, resulting in an excitation path length of 2 mm. Unfolding of holoflavodoxin in the absence of excess FMN was also followed by recording the FMN fluorescence at 525 nm with a slit of 2.5 nm for a period of 5 s.

A four-state model for equilibrium unfolding (*holoflavodoxin* ⇔ *native apoflavodoxin+FMN* ⇔ I_1*+FMN* ⇔ *unfolded apoflavodoxin+FMN*; see "Results and Discussion") was fitted globally to the unfolding data of apoflavodoxin, holoflavodoxin, and holoflavodoxin with 100 μM excess FMN using ProFit. Each GuHCl-induced equilibrium unfolding curve as observed by fluorescence or CD spectroscopy is described by Equation 3

$$Y_{obs} = \sum_j (\alpha_j + \beta_j[D])[j] \qquad \text{(Eq. 3)}$$

where α_j is the molar spectroscopic property of species j in a specific unfolding curve in the absence of denaturant, β_j describes the dependence of the molar spectroscopic property on the concentration denaturant, [D]. The observed spectroscopic signal Y (*i.e.* fluorescence or CD intensity) is the summation of contributions of all components, j (*i.e. holoflavodoxin, native apoflavodoxin,* I_1, and *unfolded flavodoxin*). The fractional population [j] of species j in a specific unfolding experiment and at a specific denaturant concentration is determined by the global fit of the four-state model described above. The spectroscopic properties of a particular protein species in different experiments are identical. However, the spectroscopic properties detected of a particular species differ slightly between different experiments. This effect is due to the concentration of free FMN that differs between the experiments. For example, FMN absorbs light, and as a result the fluorescence emission of unfolded apoflavodoxin in the presence of FMN in an unfolding experiment is slightly less compared with that of an unfolding experiment in which no FMN is present. As a consequence, the spectroscopic parameters were treated as local parameters in the fitting routine (see below for exceptions). To properly weigh each data point in the global fitting procedure, all unfolding curves were recorded with the same number of data points and each data point was weighted according to the corresponding standard error.

Native apoflavodoxin hardly populates in holoflavodoxin unfolding experiments. Consequently, in these holoflavodoxin unfolding experiments the spectroscopic properties of native apoflavodoxin (*i.e.* the α- and β-values in Equation 3) could not be determined. However, the latter spectroscopic parameters could be accurately determined in the apoflavodoxin unfolding experiment. We assumed that these parameters do not depend on the presence of holoflavodoxin or of free FMN. In the global fit of all unfolding data the α-values, as well as the β-values, of native apoflavodoxin were set to be equal. Their fitted values were mainly determined by the apoflavodoxin unfolding experiment.

The denaturant concentration dependence of the spectroscopic properties of a specific species (*i.e.* the β-values in Equation 3) can be determined accurately only when the species populates for 100% over a significant range of denaturant concentrations. However, the equilibrium folding intermediate I_1 does not populate for 100%, and thus the denaturant dependence of its CD and fluorescence intensity (*i.e.* β-values) cannot be determined. Therefore, the β-values of I_1 are fixed to 0 (13).

Denaturant Dependence of Holoflavodoxin Folding Kinetics—Folding kinetics of holoflavodoxin were measured by monitoring the FMN binding to folding apoflavodoxin molecules at 25 °C. Unfolded apoflavodoxin in 3.0 M GuHCl and a solution of FMN, both in 100 mM potassium pyrophosphate, pH 6.0, were mixed in a BioLogic SFM-4 stopped-flow machine to a final FMN concentration of 10 μM, a final protein concentration of 1.0 μM, and GuHCl concentrations ranging between 0.3 and 1.2 M. To determine the fluorescence intensity of unbound FMN in this denaturant range, blank experiments were performed without apoflavodoxin. Binding of FMN to apoflavodoxin was monitored via the accompanying quenching of FMN fluorescence. The excitation wavelength was 446 nm using an 8-nm slit and recording emission above 475 nm using a cutoff filter. Kinetic traces were fitted to exponential equations using ProFit.

The influence of Xaa-Pro peptide bond isomerization on the observed holoflavodoxin folding kinetics was examined by repeating the experiment described above with freshly unfolded apoflavodoxin, which has all Xaa-Pro peptide bonds in the native *trans* conformation. This was achieved by using a double-jump stopped-flow experiment in which native apoflavodoxin was first unfolded for a period of 600 ms in 3.0 M GuHCl. The resulting freshly unfolded apoflavodoxin solution was subsequently immediately mixed with 100 mM potassium pyrophosphate, pH 6.0, containing FMN to final concentrations of 10 μM FMN, 1.0 μM apoflavodoxin, and 0.5 M GuHCl.

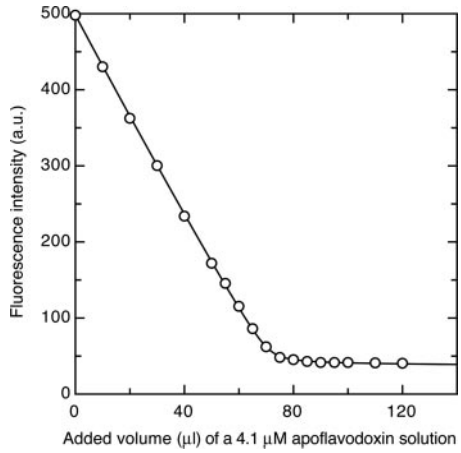

FIG. 2. **Determination of the dissociation constant of the *A. vinelandii* apoflavodoxin-FMN complex using the quenching of FMN fluorescence upon its binding to apoflavodoxin.** A 210-nM FMN solution was titrated with aliquots of a 4.1-μM apoflavodoxin solution. Equation 2 is fitted to the resulting fluorescence intensity data as described under "Experimental Procedures." The dissociation constant is determined to be (3.4 ± 0.6) 10^{-10} M in 100 mM potassium pyrophosphate, pH 6.0, at 25 °C.

Denaturant Dependence of Holoflavodoxin Unfolding Kinetics—The denaturant dependence of the unfolding kinetics of holoflavodoxin was measured by mixing holoflavodoxin and GuHCl solutions, both in 100 mM potassium pyrophosphate, pH 6.0, in a BioLogic SFM-4 stopped-flow machine to a final protein concentration of 1.0 μM and final GuHCl concentrations that range between 3.5 and 5.7 M. Unfolding of holoflavodoxin was monitored by the release of FMN, which results in a strong increase of the FMN fluorescence intensity. The samples were excited at 446 nm using an 8-nm slit, and emission was recorded above 475 nm using a cutoff filter.

RESULTS AND DISCUSSION

Dissociation Constant of the A. vinelandii Apoflavodoxin-FMN Complex—The FMN dissociation constant of *A. vinelandii* holoflavodoxin in 100 mM potassium pyrophosphate at pH 6.0 is determined by a procedure in which aliquots of apoflavodoxin are titrated to an FMN solution (see "Experimental Procedures"). In this procedure, use is made of the quenching of FMN fluorescence upon its binding to apoflavodoxin (19, 20). The corresponding binding curve is shown in Fig. 2, and the fitted dissociation constant turns out to be (3.4 ± 0.6) 10^{-10} M. This value is identical within error to the reported value of (4.4 ± 0.9) 10^{-10} M for *A. vinelandii* apoflavodoxin in 50 mM sodium phosphate at pH 7.0 (21).

Model Used to Describe Denaturant-induced A. vinelandii Holoflavodoxin Unfolding—The GuHCl-induced equilibrium unfolding of *A. vinelandii* apoflavodoxin is a three-state process and involves the population of an intermediate as shown in Equation 4

$$Apo \rightleftarrows I_1 \rightleftarrows U \qquad \text{(Eq. 4)}$$

with *Apo* being native apoflavodoxin, I_1 the folding intermediate with molten globule-like characteristics (11, 13), and U the unfolded protein. The kinetic apoflavodoxin folding intermediate I_2 (Equation 1) is not incorporated in Equation 4 as it is shown not to populate to a detectable level during denaturant-induced equilibrium unfolding of apoflavodoxin (13). Consequently, if FMN would only bind to native apoflavodoxin, holoflavodoxin denaturant-induced equilibrium unfolding would be expected to be a four-state process as shown in Equation 5

$$Holo \rightleftarrows Apo + FMN \rightleftarrows I_1 + FMN \rightleftarrows U + FMN \quad \text{(Eq. 5)}$$

with *Holo* being holoflavodoxin.

Equation 5 involves three equilibrium constants as shown in Equation 6

$$K_1 = [Holo]/[Apo][FMN] \quad K_2 = [Apo]/[I_1] \quad K_3 = [I_1]/[U] \quad \text{(Eq. 6)}$$

in which K_1 is the inverse of the dissociation constant K_D of the apoflavodoxin-FMN complex determined above. The denaturant concentration dependence of these equilibrium constants is given by Equation 7

$$K_i(D) = K_i(0)\exp(m_i[D]/RT) \quad \text{(Eq. 7)}$$

in which $[D]$ represents the denaturant concentration, $K_i(0)$ is the equilibrium constant (*i.e.* K_1, K_2, or K_3 of Equation 6) in the absence of denaturant, m_i is a constant of proportionality that describes the denaturant dependence of the equilibrium constant K_i, R is the gas constant, and T is the absolute temperature. Each equilibrium constant in Equation 6 is related to a free energy difference ΔG as shown in Equation 8.

$$\Delta G_i = -RT\ln(K_i) = -RT\ln(K_i(0)) - m_i[D] \quad \text{(Eq. 8)}$$

The concentration of free FMN in solution affects the ratio between apo- and holoflavodoxin concentrations according to Equation 6. Consequently, the apparent stability of holoflavodoxin against unfolding, ΔG^{app}_{unf}, depends on the concentration of free FMN, as is expressed in Equation 9 (22)

$$\Delta G^{app}_{unf} = \Delta G_{apo} - RT\ln\left(1 + \frac{[FMN]}{K_D}\right) \quad \text{(Eq. 9)}$$

in which ΔG_{apo} is the global stability of native apoflavodoxin. Upon denaturant-induced unfolding of a fraction of the holoflavodoxin molecules, FMN is released and this affects the apparent stability of the remaining holoflavodoxin molecules according to Equation 9. Ignoring the latter phenomenon in the analysis of equilibrium unfolding data of a ligand-binding protein will result in wrong stability values.

Denaturant-induced Unfolding Shows That A. vinelandii Holoflavodoxin Unfolds according to a Four-state Process—Because holoflavodoxin equilibrium unfolding is expected to be a four-state process (Equation 5), it is not likely that the stabilities and corresponding *m*-values of all the species involved can be extracted from a single equilibrium unfolding experiment. To determine these parameters, unfolding curves of apoflavodoxin, holoflavodoxin, and holoflavodoxin with 100 μM FMN (*i.e.* a 25-fold excess of FMN relative to holoflavodoxin) were determined. This excess of FMN ensures a virtually constant FMN concentration during denaturant-induced holoflavodoxin unfolding and contributes 7.43 kcal/mol to the holoflavodoxin stability in the absence of denaturant (Equation 9).

The GuHCl-induced equilibrium unfolding data were obtained by using tryptophan fluorescence (Fig. 3, *A* and *B*), FMN fluorescence (Fig. 3*C*), and CD spectroscopy (Fig. 3*D*). All unfolding curves were analyzed globally employing the four-state unfolding model discussed (Equation 5; also see "Experimental Procedures"). The dissociation constant $(K_1)^{-1}$ (Equation 6) is fixed at zero molar denaturant to 3.4 10^{-10} M as determined above. In the case of holoflavodoxin unfolding without excess FMN, the free FMN concentration is set to equal the total protein concentration (*i.e.* 4 μM) minus the actual concentration of holoflavodoxin. In case of holoflavodoxin unfolding with excess FMN, the free FMN concentration is fixed to 100 μM. In our analysis both unfolded flavodoxin and the flavodoxin folding intermediate I_1 did not interact to a significant extent with FMN as is experimentally supported below. Thus, the stabilities of native apoflavodoxin and of its folding intermediate I_1, both relative to unfolded apoflavodoxin, do not change between the three flavodoxin equilibrium unfolding experiments.

Identical fluorimeter settings are used to record the unfolding curves of apoflavodoxin and of holoflavodoxin without excess FMN. These settings need to be altered in case of holoflavodoxin unfolding with excess FMN because of the high optical density of FMN at 280 nm. Therefore, the fluorescence intensity values of holoflavodoxin with excess FMN cannot be directly compared with those of apoflavodoxin and holoflavodoxin in Fig. 3*A*.

All four flavodoxin unfolding curves determined by fluorescence spectroscopy are well described by the four-state unfolding model (Equation 5) as the global fit results show (Fig. 3, *A–C*). Native holoflavodoxin without excess FMN is less fluorescent than native apoflavodoxin (Fig. 3*A*) as the tryptophan fluorescence in holoflavodoxin is quenched due to the bound FMN molecule. Upon unfolding of apo- and holoflavodoxin, virtually identical fluorescence intensity values at 350 nm were obtained (Fig. 3, *A* and *B*). The small differences observed were most likely caused by the absorption of free FMN at 280 nm. This showed that FMN does thus not interact to a significant extent with unfolded flavodoxin.

The excellent fit of the four-state unfolding model to the 350-nm as well as the 525-nm fluorescence data showed that, indeed, FMN does not significantly interact with I_1 or with unfolded flavodoxin. In the case of holoflavodoxin without excess FMN a hump is observed at 2.6 M GuHCl in its unfolding curve measured by tryptophan fluorescence (Fig. 3*B*). This hump is caused by the population of I_1 and its fluorescence properties. FMN does not interact to a significant extent with I_1 as supported by the monitoring of holoflavodoxin unfolding without excess FMN via the fluorescence intensity of FMN at 525 nm (Fig. 3*C*). At this wavelength FMN gives a high fluorescence intensity when free in solution, whereas the fluorescence of FMN bound to holoflavodoxin is quenched. Note that the hump in the 350-nm tryptophan fluorescence data (Fig. 3*B*) is not observed in the 525-nm flavin fluorescence data, which shows that I_1, just as *U*, does not interact with FMN.

All three flavodoxin unfolding curves determined by CD at 222 nm (Fig. 3*D*) are also well described by the four-state unfolding model (Equation 5). Native holoflavodoxin without excess FMN gives a stronger CD signal at 222 nm than native apoflavodoxin (Fig. 3*D*). This is attributed to the formation of some secondary structure in the FMN binding site of flavodoxin upon binding of FMN (5, 6). Unfolded apo- and holoflavodoxin have virtually identical ellipticity values (Fig. 3*D*). This supports that the presence of FMN does not affect the conformation of unfolded flavodoxin. In the case of holoflavodoxin with 100 μM excess FMN, the ellipticity at 222 nm is 1 millidegree less negative compared with the ellipticity of holoflavodoxin without excess FMN (Fig. 3*D*). This difference is attributed to the ellipticity of 100 μM free FMN, which gives a positive CD signal at 222 nm of 1 millidegree (data not shown).

The results of the global fit of Equation 5 to the flavodoxin unfolding data are summarized in Table I. The equilibrium populations of holoflavodoxin, native apoflavodoxin, I_1, and of unfolded flavodoxin, with and without 100 μM excess FMN, are shown in Fig. 4 as a function of denaturant concentration. In summary, the denaturant-induced unfolding experiments show that equilibrium unfolding of *A. vinelandii* holoflavodoxin is well described by the four-state unfolding model *holoflavodoxin* $\Leftrightarrow$ *native apoflavodoxin*+*FMN* $\Leftrightarrow$ I_1+*FMN* $\Leftrightarrow$ *unfolded apoflavodoxin*+*FMN*.

Global Stability of Holoflavodoxin—The stabilities of native apoflavodoxin and of the folding intermediate I_1 and corre-

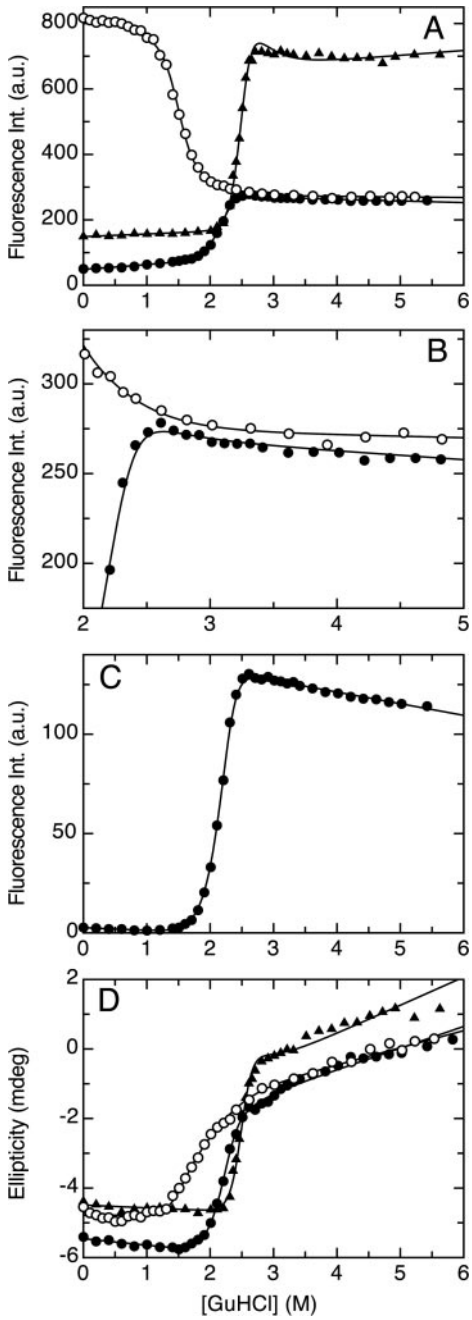

FIG. 3. **GuHCl-induced equilibrium unfolding data of *A. vinelandii* flavodoxin.** The *solid lines* are the results of a global fit of a four-state unfolding model (*holoflavodoxin* ⇔ *native apoflavodoxin* + *FMN* ⇔ I_1+*FMN* ⇔ *unfolded apoflavodoxin*+*FMN*, Equation 5) to all data presented, as described in the main text. In this model, FMN is either bound to the protein to form holoflavodoxin or it is free in solution. *A*, the unfolding of apoflavodoxin (O), holoflavodoxin (●), and of holoflavodoxin with 100 μM excess FMN (▲) as monitored by tryptophan fluorescence at 350 nm. The fluorescence intensity values of the samples of holoflavodoxin with 100 μM FMN cannot be directly compared with those of the apoflavodoxin and holoflavodoxin samples as the excess of FMN leads to a high optical density of the corresponding samples at the excitation wavelength used and thus requires modified spectrometer settings. *B*, zoom-in graph of the apoflavodoxin (O) and holoflavodoxin (●) data presented in *panel A* that shows the hump that resides at the high denaturant concentration part of the transition zone of the unfolding curve of holoflavodoxin. This hump is caused by the population of I_1 and its fluorescence properties. *C*, unfolding of holoflavodoxin without excess FMN as monitored by FMN fluorescence at 525 nm. Note that the hump seen in *panel B* is not present here as I_1, just as U, does not interact with FMN. *D*, the monitoring by CD at 222 nm of the unfolding of apoflavodoxin (O), holoflavodoxin (●), and of holoflavodoxin with 100 μM excess FMN (▲). The unfolding experiments are done at 25 °C in 100 mM potassium pyrophosphate, pH 6.0, and the protein concentration is 4.0 μM.

sponding denaturant concentration dependences (*i.e. m*-values) presented in Table I are within error identical to values reported previously for denaturant-induced apoflavodoxin (un)folding (13). However, the seven unfolding curves presented here result in much lower fitting errors. The recording of unfolding curves of flavodoxin at different FMN concentrations (*i.e.* no FMN present, with equimolar amounts of FMN, and with excess FMN) together with the determination of the holoflavodoxin dissociation constant is a powerful approach to determine the stability of apo- and holoflavodoxin with high accuracy. A similar approach, in which the ligand concentration is varied, can be used to accurately determine the stability of other ligand-binding proteins.

The stability of a cofactor-binding protein is expected to equal the sum of the stability of the apoprotein and the free energy that is gained upon binding of the cofactor (22). Wittung-Stafshede and co-workers (23) propose that FMN binding has no effect on the denaturant-induced equilibrium unfolding of *Desulfovibrio desulfuricans* flavodoxin, whereas the presence of FMN speeds up the folding of this protein (24). The resulting thermodynamic conflict is handled by Wittung-Stafshede and co-workers by assuming that unfolded *D. desulfuricans* flavodoxin binds to FMN with nanomolar affinity, which is a rather remarkable assumption.

In contrast, the results presented here show that the presence of FMN has a clear effect on the denaturant-induced equilibrium unfolding of *A. vinelandii* flavodoxin (Fig. 3, *A* and *D*). Apo- and holoflavodoxin start to unfold at largely different concentrations of denaturant, and no appreciable interaction between FMN and unfolded apoflavodoxin molecules is observed. In addition, kinetic holoflavodoxin folding experiments showed that FMN does not accelerate *A. vinelandii* flavodoxin folding (see "The Kinetics of *A. vinelandii* Holoflavodoxin Folding"). The equilibrium unfolding data of *A. vinelandii* flavodoxin are described by a four-state folding model (Equation 5) in which only native apoflavodoxin interacts with FMN. Consequently, we concluded that in accordance with thermodynamic theory the global stability of *A. vinelandii* holoflavodoxin equals the sum of the global stability of apoflavodoxin and the free energy associated with FMN binding to native apoflavodoxin. The global stability of *A. vinelandii* holoflavodoxin in the presence of 100 μM FMN is 10.16 + 7.43 = 17.59 kcal/mol (Table I, Equation 9).

The Kinetics of FMN Binding to A. vinelandii Apoflavodoxin Involve Two Rate Constants—The kinetics of FMN binding to apoflavodoxin were determined at different protein concentrations. Pseudo-first-order kinetics were obtained by using at least a 10-fold excess of apoflavodoxin relative to FMN. In Fig. 5*A* a fluorescence intensity trace of FMN mixed with native apoflavodoxin is shown. A sum of two exponentials is required to properly describe the data (Fig. 5, *B* and *C*). Two rate constants for FMN binding to apoflavodoxin were observed at all protein concentrations used, with both rate constants linearly depending on the protein concentration (Fig. 6*A*). In addition, two distinct rate constants for FMN binding were also observed at all GuHCl concentrations at which apoflavodoxin is still native (*i.e.* up to 1.0 M GuHCl) (data not shown). The larger binding rate constant is associated with a large amplitude (93 ± 2% of the total signal on average), whereas the slower binding process contributes for 7 ± 2% to the observed FMN binding kinetics (Fig. 6*B*). The small amplitude associated with the slower binding process causes the observed scatter in the corresponding binding rate constants (Fig. 6*A*). Second-order rate constants for FMN binding to excess *A. vinelandii* apoflavodoxin of 0.95 ± 0.02 and 0.27 ± 0.03 $\mu M^{-1}\ s^{-1}$, respectively, were derived from the protein concentration dependence of

TABLE I

Thermodynamic parameters obtained from the GuHCl-induced equilibrium unfolding of A. vinelandii holoflavodoxin

A four-state model for equilibrium unfolding (*holoflavodoxin* ⇔ *native apoflavodoxin* + *FMN* ⇔ I_1 + *FMN* ⇔ *unfolded apoflavodoxin* + *FMN*, Equations 3–7) is fitted to the unfolding data of apoflavodoxin, holoflavodoxin, and of holoflavodoxin with 100 μM excess FMN (see "Results and Discussion"). The free energy differences in the absence of denaturant (ΔG) and corresponding denaturant concentration dependencies (m) are given for the equilibrium between unfolded flavodoxin U and the apoflavodoxin folding intermediate I_1 (ΔG_{UI} and m_{UI}), for the equilibrium between intermediate I_1 and native apoflavodoxin (ΔG_{IA} and m_{IA}), for the equilibrium between unfolded and native apoflavodoxin (ΔG_{UA} and m_{UA}), and for the equilibrium between native apo- and holoflavodoxin in the theoretical presence of 1 M FMN (ΔG_b and m_b), respectively. The errors given are standard fitting errors.

ΔG_{UI}	(kcal/mol)	−3.47 ± 0.05	m_{UI}	(kcal/mol·M^{-1})	−1.84 ± 0.01
ΔG_{IA}	(kcal/mol)	−6.69 ± 0.01	m_{IA}	(kcal/mol·M^{-1})	−4.38 ± 0.02
ΔG_{UA}	(kcal/mol)	−10.16 ± 0.06	m_{UA}	(kcal/mol·M^{-1})	−6.22 ± 0.02
ΔG_b	(kcal/mol)	−12.86[a]	m_b	(kcal/mol·M^{-1})	−0.79 ± 0.01

[a] $RT\ln(K_D)$, with K_D = 3.4 10^{-10} M, the value determined for the FMN dissociation constant of *A. vinelandii* holoflavodoxin based on the data presented in Figure 2.

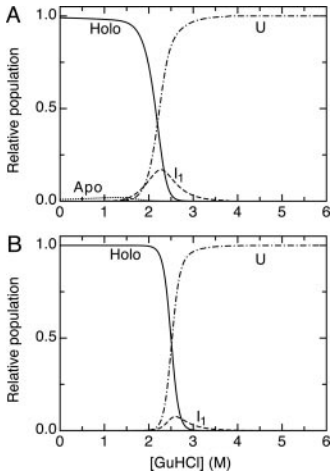

FIG. 4. **Normalized equilibrium population of holoflavodoxin (*solid line*), native apoflavodoxin (*dotted line*), folding intermediate I_1 (*dashed line*), and unfolded apoflavodoxin (*dash-dotted line*) during the equilibrium unfolding of holoflavodoxin without excess FMN (*A*) and with 100 μM excess FMN (*B*), respectively.** The populations are derived from the results of the four-state global fit to the experimental flavodoxin unfolding data shown in Fig. 3 and summarized in Table I.

both FMN binding rate constants (Fig. 6*A*). The errors on the second-order rate constants were estimated using a Chi-squared test (25).

What causes the observed bi-exponential FMN binding kinetics of *A. vinelandii* apoflavodoxin? In the case of *Desulfovibrio vulgaris* apoflavodoxin monophasic FMN binding kinetics are observed in the absence of inorganic phosphate in the buffer, whereas in the presence of phosphate FMN binding is biphasic (26). Based on these observations and additional studies (27) it was proposed that in the absence of free phosphate the 5′-phosphate of FMN binds first to apoflavodoxin followed by binding of the isoalloxazine ring. Inorganic phosphate was proposed to bind to the phosphate binding site of a fraction of the *D. vulgaris* apoflavodoxin molecules, leading to a preformed isoalloxazine binding site (26). The latter allows the isoalloxazine ring of FMN to bind first to apoflavodoxin in these molecules. Consequently, biphasic FMN binding kinetics were observed for *D. vulgaris* apoflavodoxin in the presence of phosphate. The slower kinetic phase was assigned to the phosphate-first binding mode and the faster phase to the ring-first binding mode (26).

The studies of Murray and Swenson (26) prompted us to determine the amount of free inorganic phosphate in the buffer we used (*i.e.* 100 mM potassium pyrophosphate). ^{31}P NMR spectroscopy showed that ~2% of the ^{31}P nuclei present in this buffer is present as phosphate (data not shown). Thus ~4 mM inorganic phosphate is present in the FMN binding studies of *A. vinelandii* apoflavodoxin. Most likely, the bi-exponential FMN binding kinetics of *A. vinelandii* apoflavodoxin are caused by the binding of inorganic phosphate to the phosphate binding site of a fraction of the *A. vinelandii* apoflavodoxin molecules. The slower kinetic phase observed would be due to the phosphate-first binding mode of FMN to *A. vinelandii* apoflavodoxin molecules that contain no inorganic phosphate. *A. vinelandii* apoflavodoxin molecules that have an inorganic phosphate ion bound would cause the faster kinetic phase observed due to the ring-first binding mode of FMN to these molecules, just as is observed for *D. vulgaris* apoflavodoxin (26).

The Rate of FMN Release Determines the A. vinelandii Holoflavodoxin Unfolding Rate—Holoflavodoxin unfolding is measured via the corresponding release of FMN, which results in a strong increase of its fluorescence intensity (Fig. 7*A*). At each GuHCl concentration studied (*i.e.* 3.5–5.7 M GuHCl), only one unfolding rate constant was observed (Fig. 7*B*). Clearly, the natural logarithm of the holoflavodoxin unfolding rate constant depends linearly on the GuHCl concentration. The linear extrapolation of the holoflavodoxin unfolding rate constants presented in Fig. 7*B* to 0 molar GuHCl leads to a holoflavodoxin unfolding rate constant in water of (8.9 ± 0.8) 10^{-5} s^{-1}, and the corresponding m-value is 0.65 ± 0.01 kcal/mol·M^{-1}. The errors on the rate constant and m-value were estimated using a Chi-squared test (25).

It was previously suggested based on hydrogen/deuterium exchange results that FMN release is probably the rate-limiting step in *A. vinelandii* holoflavodoxin unfolding (5, 28), as is also observed for *D. vulgaris* holoflavodoxin unfolding (29). If true, the *A. vinelandii* holoflavodoxin unfolding rate constant should equal the rate constant for FMN release from holoflavodoxin. The rate constant for FMN release can be deduced using the rate constant for FMN binding to *A. vinelandii* apoflavodoxin and the dissociation constant of the apoflavodoxin-FMN complex, both of which have been experimentally determined in this study. The slowest FMN binding rate constant observed (*i.e.* 0.27 ± 0.03 μM^{-1} s^{-1}) most likely results from binding of FMN to apoflavodoxin molecules that contain no inorganic phosphate ion. The dissociation constant K_D of the apoflavodoxin-FMN complex is determined to be (3.4 ± 0.6) 10^{-10} M. This dissociation constant describes the relative amounts of holoflavodoxin and apoflavodoxin at equilibrium. The rate constant for release of FMN from holoflavodoxin equals the rate constant for FMN binding to apoflavodoxin × the dissociation constant of the apoflavodoxin-FMN complex and is (9 ± 2) 10^{-5} s^{-1}. This value matches with the holoflavodoxin unfolding rate constant in water of (8.9 ± 0.8) 10^{-5} s^{-1}. Thus, FMN release is indeed the rate-limiting step in *A. vinelandii* holoflavodoxin global unfolding.

The data shown in Fig. 7*B* represent the GuHCl concentration dependence of the rate constant for FMN release from *A. vinelandii* holoflavodoxin. Extrapolation of these data shows

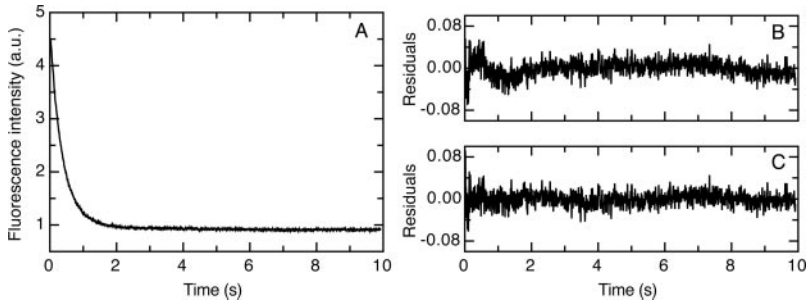

FIG. 5. **Two rate constants describe FMN binding to native *A. vinelandii* apoflavodoxin.** *A*, kinetics of FMN binding to native apoflavodoxin as monitored by the quenching of the FMN fluorescence emission above 475 nm in a stopped-flow instrument. *B*, residuals of a fit of a single exponential equation to the data. *C*, residuals of a fit of a sum of two exponential equations to the data with the fitted rate constants being 2.86 ± 0.02 and 0.98 ± 0.08 s^{-1}, respectively. The final flavodoxin concentration is 3 μM, and the final FMN concentration is 0.10 μM, both in 100 mM potassium pyrophosphate. pH 6.0, at 25 °C.

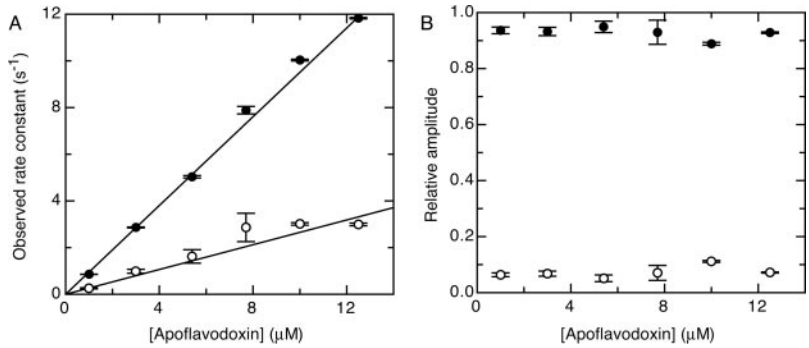

FIG. 6. **Observed rate constants for FMN binding to *A. vinelandii* apoflavodoxin as a function of the final protein concentration in 100 mM potassium pyrophosphate, pH 6.0, at 25 °C.** The final FMN concentration is 0.10 μM in all cases, except for the two highest protein concentrations used (*i.e.* 10 and 12.5 μM), where it is 1.0 μM. *A*, the protein concentration dependence of both observed rate constants is fitted to a straight line that crosses the origin; the corresponding slopes are the pseudo-first-order rate constants. The faster of the two observed FMN binding rate constants (●) fits to a pseudo-first-order rate constant of 0.95 ± 0.02 $\mu M^{-1}\ s^{-1}$, whereas the slower one (O) fits to a pseudo-first-order rate constant of 0.27 ± 0.03 $\mu M^{-1}\ s^{-1}$. *B*, relative amplitudes associated with the faster (●) and the slower (O) observed rate constants for FMN binding to apoflavodoxin as a function of the protein concentration. The *error bars* give the standard fitting errors of the rate constants and of the relative amplitudes, respectively.

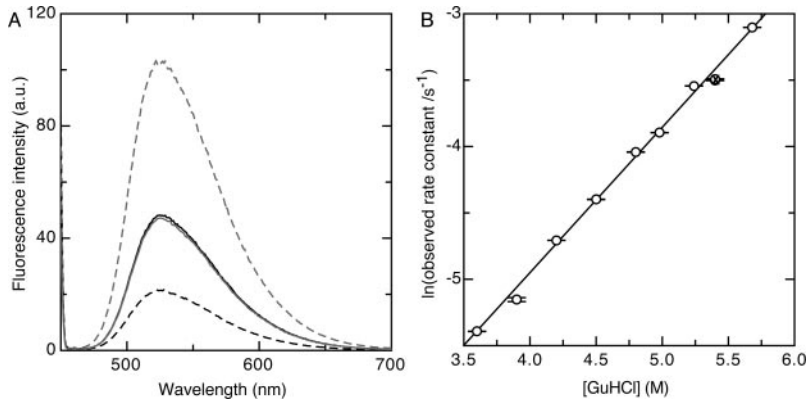

FIG. 7. **Unfolding kinetics of *A. vinelandii* holoflavodoxin monitored by FMN fluorescence emission.** *A*, fluorescence emission spectrum of free FMN (*gray lines*) and of the same concentration of FMN in the presence of an equimolar amount of *A. vinelandii* apoflavodoxin (*black lines*), showing the effect of the absence (*dashed lines*) and the presence (*solid lines*) of 4 M GuHCl. In the absence of denaturant, FMN binds to apoflavodoxin; as a result, its fluorescence intensity is strongly quenched. Apoflavodoxin is unfolded in 4 M GuHCl; as a result, the FMN fluorescence emission spectrum in the presence of an equimolar amount of apoflavodoxin and 4 M GuHCl is indistinguishable from the one of free FMN in 4 M GuHCl. Apoflavodoxin (when present) and FMN concentrations are 1 μM in 100 mM potassium pyrophosphate, pH 6.0, at 25 °C. Excitation is at 446 nm, and a 5-nm slit is used. *B*, natural logarithm of the single observed rate constant for *A. vinelandii* holoflavodoxin unfolding (O) as a function of the GuHCl concentration. At the *X* sign two data points overlap. The *solid line* is the result of a linear fit to all data shown. The unfolding rate constant extrapolated to water is (8.9 ± 0.8) $10^{-5}\ s^{-1}$, and the corresponding *m*-value is 0.65 ± 0.01 kcal/mol·M^{-1}. The *error bars* show the standard errors of the rate constants. The experiments are done at 25 °C, and final conditions are 1.0 μM flavodoxin in 100 mM potassium pyrophosphate, pH 6.0.

that in the absence of denaturant *A. vinelandii* holoflavodoxin unfolds approximately once every 3 h.

The Kinetics of A. vinelandii Holoflavodoxin Folding—The folding kinetics of apoflavodoxin from *A. vinelandii* in the absence of FMN have been studied in great detail (13). Single-jump and interrupted refolding experiments showed that the refolding kinetics of *A. vinelandii* apoflavodoxin are complex and involve four processes, with rate constants λ_1 to λ_4 in order of decreasing value. All four processes yield native apoflavodoxin molecules. The fastest process with rate constant λ_1 corresponds to the rapid formation of native apoflavodoxin along the most direct folding route from unfolded to native

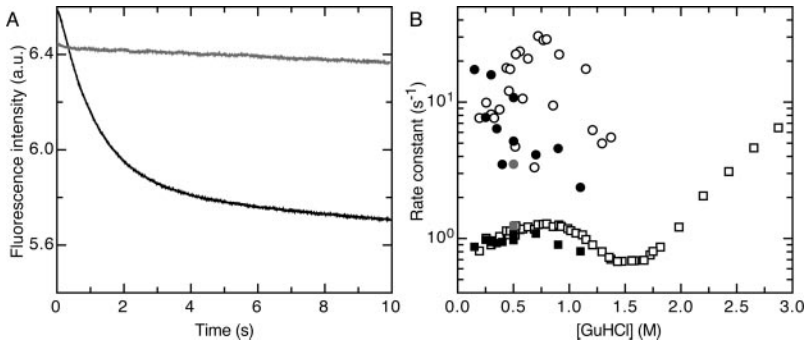

FIG. 8. **Folding kinetics of *A. vinelandii* holoflavodoxin.** *A*, time-dependent fluorescence intensity resulting from FMN binding to folding *A. vinelandii* apoflavodoxin molecules (*black line*) detected via the quenching of the FMN fluorescence above 475 nm. The trace is obtained by mixing unfolded apoflavodoxin (in 3.0 M GuHCl) with buffer containing FMN to final conditions of 10 μM FMN, 1.0 μM flavodoxin, 0.50 M GuHCl, 100 mM potassium pyrophosphate, pH 6.0, at 25 °C. Under these final conditions apoflavodoxin is in its native state. The *gray line* shows the trace obtained when repeating the same experiment in the absence of protein. The steady decrease in fluorescence emission observed in the latter trace is caused by the time-dependent photobleaching of FMN. *B*, chevron plot of the two largest observed rate constants for *A. vinelandii* holoflavodoxin folding as observed by changes in FMN fluorescence above 475 nm (●, λ_1; ■, λ_2). For comparison, the corresponding *A. vinelandii* apoflavodoxin folding rate constants as observed by changes in tryptophan fluorescence intensity are shown as well (open symbols). The two smallest folding rate constants for both apo- and holoflavodoxin folding (*i.e.* λ_3 and λ_4) are not shown as they do not inform about the folding mechanism of flavodoxin, because they originate from Xaa-Pro peptide bond isomerizations. Up to 0.7 M GuHCl, the folding rate constants observed for both holo- and apoflavodoxin are identical within error. The λ_1 and λ_2 rate constants for refolding of freshly unfolded apoflavodoxin (made by unfolding apoflavodoxin for a period of 600 ms in 3.0 M GuHCl) in the presence of FMN at 0.5 M GuHCl are shown in *gray*. The rate constants are plotted on a logarithmic scale. Final conditions are 1.0 μM flavodoxin in 100 mM potassium pyrophosphate, pH 6.0, at 25 °C. In the case of holoflavodoxin, 10 μM FMN is present as well. Apoflavodoxin folding data are taken from Ref. 13.

protein. Only a small fraction (11%) (13) of the folding apoflavodoxin molecules follows the direct folding route. On this route (unfolded apoflavodoxin $\Leftrightarrow I_2 \Leftrightarrow$ native apoflavodoxin), a high energy intermediate I_2 is transiently formed. The process with rate constant λ_2 corresponds to the formation of native apoflavodoxin via a relatively stable intermediate I_1 ($I_1 \Leftrightarrow$ unfolded apoflavodoxin $\Leftrightarrow I_2 \Leftrightarrow$ native apoflavodoxin, Equation 1). The unfolding of the latter intermediate is the rate-limiting step in the formation of native apoflavodoxin with rate constant λ_2. The two slowest folding processes (with rate constants λ_3 and λ_4) are because of Xaa-Pro peptide bond isomerizations in the unfolded state (13).

In this study the influence of FMN on the folding kinetics of *A. vinelandii* flavodoxin was investigated. Unfolded apoflavodoxin in 3.0 M GuHCl was mixed into buffer containing FMN, and the subsequent binding of FMN to the folding apoflavodoxin molecules was monitored, as shown in Fig. 8*A*. A sum of three exponential equations was needed to properly fit the time-dependent fluorescence signal obtained, which led to the identification of three observable folding rate constants.

The slowest folding rate constant observed in the holoflavodoxin folding experiment is equal to λ_3 observed during apoflavodoxin kinetic folding, which originates from Xaa-Pro peptide bond isomerizations (a rate constant of ~0.3 s^{-1}, data not shown). The slowest apoflavodoxin folding rate constant λ_4 of 0.03 s^{-1} in the absence of denaturant, which also originates from Xaa-Pro peptide bond isomerizations, cannot be extracted from the data. Rate constant λ_4 was not sufficiently sampled in the holoflavodoxin kinetic folding traces, as these traces were recorded for a period of only 10 s. As both λ_3 and λ_4 originate from Xaa-Pro peptide bond isomerizations, they do not inform about the folding mechanism of both apo- and holoflavodoxin.

The dependence of the two fastest rate constants for both apoflavodoxin folding and holoflavodoxin folding (*i.e.* λ_1 and λ_2) on the GuHCl concentration is shown in Fig. 8*B*. Up to 0.7 M GuHCl, the rate constants for holoflavodoxin folding as observed via FMN binding are identical within error to those observed for apoflavodoxin folding. Clearly, excess FMN does not accelerate flavodoxin folding, and FMN thus does not act as a nucleation site for flavodoxin folding. Instead, in the presence of excess FMN, formation of native apoflavodoxin is the rate-limiting process in the folding of *A. vinelandii* holoflavodoxin.

Above 0.7 M GuHCl, the FMN binding rate constants deviated from the apoflavodoxin folding rate constants. At these concentrations of denaturant both folding and unfolding processes contributed to the observed kinetics, and as holoflavodoxin unfolds slower than apoflavodoxin, the resulting observed rate constants for holoflavodoxin folding were lower than those of apoflavodoxin folding.

The largest folding rate observed during apoflavodoxin folding (*i.e.* λ_1) contains contributions from the formation of folding intermediates with non-native Xaa-Pro peptide bond isomers (13). In case these intermediates are able to bind FMN, this could influence the observed holoflavodoxin folding kinetics as monitored by FMN binding (Fig. 8*B*). However, freshly unfolded apoflavodoxin gave upon folding in the presence of FMN at 0.5 M GuHCl rate constants for FMN binding that were identical within error to the rate constants for folding of equilibrium unfolded apo- and holoflavodoxin (Fig. 8*B*). In freshly unfolded apoflavodoxin (made by unfolding apoflavodoxin for 600 ms in 3.0 M GuHCl) the vast majority of the Xaa-Pro peptide bond isomers was native. Hence, apoflavodoxin folding intermediates with non-native Xaa-Pro peptide bonds did not bind FMN.

In Fig. 8*A* the time-dependent fluorescence intensity of free FMN in a kinetic folding experiment is shown, recorded under identical circumstances as for holoflavodoxin folding, except that now no protein was present. The initial fluorescence intensity of FMN during kinetic holoflavodoxin folding was somewhat (2%) higher than observed in the blank experiment in which flavodoxin was absent. This higher intensity might suggest a weak association of FMN with the folding apoflavodoxin molecules, which would result in FMN being less accessible to GuHCl compared with unbound FMN. We observed that the fluorescence intensity of free FMN was quenched by the presence of GuHCl (24% quenching at 0.5 M GuHCl, data not shown).

No indications for the association of FMN with apoflavodoxin unfolded in 4 M GuHCl were observed. First, at this denaturant concentration the fluorescence emission spectra of FMN in the presence and in the absence of apoflavodoxin were identical (Fig. 7*A*). Second, ^{1}H NMR spectra of holoflavodoxin unfolded in 4 M GuHCl showed sharp resonances of FMN protons at frequencies that coincided within the spectral resolution of 0.01

ppm with those of FMN in 4 M GuHCl in the absence of flavodoxin (data not shown). Third, the observed flavodoxin folding kinetics were not affected by the presence of excess FMN (Fig. 8*B*). Fourth, the holoflavodoxin denaturant-induced equilibrium unfolding data (Fig. 3) were excellently described by assuming that only native apoflavodoxin binds FMN. In summary, if any association of FMN with unfolded apoflavodoxin molecules exists, it must be weak.

FMN did not associate with the apoflavodoxin folding intermediate I_1 as well. Up to 0.7 M GuHCl the observed flavodoxin folding kinetics were not affected (Fig. 8*B*): λ_2 increased with increasing denaturant concentration for both apo- and holoflavodoxin. This increase reflects the unfolding of the off-pathway apoflavodoxin folding intermediate I_1 (13). As the presence of FMN leads to no alteration in the latter phenomenon, binding of FMN to I_1 seems unlikely. As discussed, the latter is supported by the holoflavodoxin equilibrium unfolding data being well described by assuming that only native apoflavodoxin binds FMN to a significant extent. In accordance, at 2.6 M GuHCl, where I_1 is populated for 11.7% whereas native holoflavodoxin is populated for less than 1% (Fig. 4*A*), the entire fluorescence emission spectra (ranging from 475 to 675 nm) of FMN in the presence and in the absence of apoflavodoxin were identical (data not shown). In summary, the off-pathway intermediate I_1 does not bind FMN with an appreciable binding constant. In addition, the high energy on-pathway intermediate I_2 (Equation 1) exists for such a short time (13) that FMN binding to this intermediate must also be negligible.

Under the conditions investigated the formation of native apoflavodoxin molecules was the rate-limiting step in *A. vinelandii* holoflavodoxin folding. Therefore, FMN binding to native apoflavodoxin must be the final step in *A. vinelandii* holoflavodoxin folding. Taking all observations together, the kinetic model for *A. vinelandii* apoflavodoxin folding can now be extended to describe kinetic holoflavodoxin folding: I_1 + *FMN* ⇔ *unfolded apoflavodoxin* + *FMN* ⇔ I_2 + *FMN* ⇔ *native apoflavodoxin* + *FMN* ⇔ *holoflavodoxin*.

CONCLUSION

The folding data of *A. vinelandii* holoflavodoxin have shown that first apoflavodoxin folds to its native state. FMN binding to native apoflavodoxin was the subsequent last step in holoflavodoxin folding. Flavodoxin folding was an autonomous process that *in vitro* did not require the assistance of chaperone molecules. Excess FMN did not accelerate holoflavodoxin kinetic folding, and FMN did not act as a nucleation site for flavodoxin folding. The kinetic folding of holoflavodoxin is described by I_1 + *FMN* ⇔ *unfolded apoflavodoxin* + *FMN* ⇔ I_2 + *FMN* ⇔ *native apoflavodoxin* + *FMN* ⇔ *holoflavodoxin*. No indications exist for unfolded apoflavodoxin, the molten globule-like apoflavodoxin off-pathway folding intermediate I_1, or the high energy on-pathway intermediate I_2 to interact to a significant extent with FMN. The stability of holoflavodoxin from *A. vinelandii* was so high that even under strongly denaturing conditions FMN needed to be released first before global unfolding of the protein could occur. This global unfolding is a rare event, occurring approximately once every 3 h in the absence of denaturant.

REFERENCES

1. Baker, D. (2000) *Nature* **405,** 39–42
2. Baldwin, R. L. (1996) *Folding Des.* **1,** R1–R8
3. Bieri, O., Wildegger, G., Bachmann, A., Wagner, C., and Kiefhaber, T. (1999) *Biochemistry* **38,** 12460–12470
4. Fisher, W. R., Taniuchi, H., and Anfinsen, C. B. (1973) *J. Biol. Chem.* **248,** 3188–3195
5. Steensma, E., Nijman, M. J. M., Bollen, Y. J. M., de Jager, P. A., van den Berg, W. A. M., van Dongen, W. M. A. M., and van Mierlo, C. P. M. (1998) *Protein Sci.* **7,** 306–317
6. Steensma, E., and van Mierlo, C. P. M. (1998) *J. Mol. Biol.* **282,** 653–666
7. van Berkel, W. J. H., Benen, J. A. E., and Snoek, M. C. (1991) *Eur. J. Biochem.* **197,** 769–779
8. Bertini, I., Cowan, J. A., Luchinat, C., Natarajan, K., and Piccioli, M. (1997) *Biochemistry* **36,** 9332–9339
9. Robinson, C. R., Liu, Y., Thomson, J. A., Sturtevant, J. M., and Sligar, S. G. (1997) *Biochemistry* **36,** 16141–16146
10. Hefti, M. H., Vervoort, J., and van Berkel, W. J. H. (2003) *Eur. J. Biochem.* **270,** 4227–4242
11. van Mierlo, C. P. M., van Dongen, W. M. A. M., Vergeldt, F., van Berkel, W. J. H., and Steensma, E. (1998) *Protein Sci.* **7,** 2331–2344
12. van Mierlo, C. P. M., van den Oever, J. M. P., and Steensma, E. (2000) *Protein Sci.* **9,** 145–157
13. Bollen, Y. J. M., Sánchez, I. E., and van Mierlo, C. P. M. (2004) *Biochemistry* **43,** 10475–10489
14. Bollen, Y. J. M., and van Mierlo, C. P. M. (2005) *Biophys. Chem.*, in press
15. Klugkist, J., Voorberg, J., Haaker, H., and Veeger, C. (1986) *Eur. J. Biochem.* **155,** 33–40
16. Edmondson, D. E., and Tollin, G. (1971) *Biochemistry* **10,** 124–132
17. Barman, B. G., and Tollin, G. (1972) *Biochemistry* **11,** 4746–4754
18. Mayhew, S. G., and Wassink, J. H. (1980) *Methods Enzymol.* **66,** 217–220
19. Lostao, A., Gomez-Moreno, C., Mayhew, S. G., and Sancho, J. (1997) *Biochemistry* **36,** 14334–14344
20. Mayhew, S. G. (1971) *Biochim. Biophys. Acta* **235,** 289–302
21. Pueyo, J. J., Curley, G. P., and Mayhew, S. G. (1996) *Biochem. J.* **313,** 855–861
22. Creighton, T. E. (1993) *Proteins, Stuctures, and Molecular Properties*, 2nd Ed., pp. 338–340, W. H. Freeman and Company, New York
23. Apiyo, D., Guidry, J., and Wittung-Stafshede, P. (2000) *Biochim. Biophys. Acta* **1479,** 214–224
24. Apiyo, D., and Wittung-Stafshede, P. (2002) *Protein Sci.* **11,** 1129–1135
25. Press, W. H., Teukolsky, A. A., Vetterling, W. T., and Flannery, B. P. (1992) *Numerical Recipes, the Art of Scientific Computing*, 2nd Ed., pp. 517–565, Cambridge University Press, Cambridge, UK
26. Murray, T. A., and Swenson, R. P. (2003) *Biochemistry* **42,** 2307–2316
27. Murray, T. A., Foster, M. P., and Swenson, R. P. (2003) *Biochemistry* **42,** 2317–2327
28. van Mierlo, C. P. M., and Steensma, E. (1999) *J. Mol. Catal. B Enzym.* **7,** 147–156
29. Nuallain, B. O., and Mayhew, S. G. (2002) *Eur. J. Biochem.* **269,** 212–223
30. Kraulis, P. J. (1991) *J. Appl. Crystallogr.* **24,** 946–950
31. Thorneley, R. N. F., Ashby, G. A., Drummond, M. H., Eady, R. R., Hughes, D. L., Ford, G., Harrison, P. M., Shaw, A., Robson, R. L., Kazlauskaite, J., and Hill, H. A. O. (1994) in *Flavins and Flavoproteins* (1993) (Yagi, K., ed), pp. 343–354, Walter de Gruyter & Co., Berlin